DOI: 10.1002/vms3.319

ORIGINAL ARTICLE

WILEY

Characterization of the ablation zones produced by three commercially available systems from a single vendor for radiofrequency thermoablation in an ex vivo swine liver model

Michela Bullone[1] | Roberto Garberoglio[2] | Paola Pregel[1] | Francesca T. Cannizzo[1] | Arianna Gagliardo[1] | Marina Martano[1] | Enrico Bollo[1] | Frine E. Scaglione[1]

[1]Department of Veterinary Sciences, University of Turin, Grugliasco, Italy

[2]Division of endocrinology, diabetology and metabolism - Department of Medical Sciences, University of Turin, Torino, Italy

Correspondence
Michela Bullone, Department of Veterinary Sciences, University of Turin, Largo Paolo Braccini 2, Grugliasco 10095, Italy.
Email: michelabullone@gmail.com

Funding information
This work was performed at the Department of Veterinary Science, University of Turin, Italy. It was funded by Fondazione CRT Erogazioni Ordinarie (FES, #2015.2595). The RF ablation system was kindly provided by RF Medical Co., Ltd. (Korea). RF Medical Co., Ltd. (Korea) was not involved in the study design, data analysis and interpretation. RF Medical Co., Ltd. (Korea) was not involved in manuscript writing or in the decision to submit the manuscript for publication. RF Medical Co., Ltd. (Korea) accepted the manuscript as drafted by the authors.

Abstract

Background: Radiofrequency Ablation (RFA) is rarely performed in veterinary medicine. A rationale exists for its use in selected cases of canine liver tumours. RFA induces ablation zones of variable size and geometry depending on the technique used and on the impedance of the targeted organ.

Objectives: (a) to describe the geometry and reproducibility of the ablation zones produced by three commercially available systems from a single company, using isolated swine liver parenchyma as a model for future veterinary applications in vivo; (b) to study the effects of local saline perfusion into the ablated parenchyma through the electrode tip and of single versus double passage of the electrode on size, geometry and reproducibility of the ablation zones produced.

Methods: Size, and geometry of ablation zones reproduced in six livers with one cooled and perfused (saline) and two cooled and non-perfused systems, after single or double passage (n = 6/condition), were assessed macroscopically on digitalized images by a blinded operator. Longitudinal and transverse diameters, equivalent diameter, estimated volume and roundness index were measured. Reproducibility was assessed as coefficient of variation.

Results and Conclusions: Ablation zone reproducibility was higher when expressed in terms of ablation zone diameters than estimated volume. Local saline perfusion of the parenchyma through the electrode tip during RFA increased the ablation zone longitudinal diameter. Ablation zone estimated volume increased with saline perfusion only when double passage was performed. These data may provide useful information for those clinicians who intend to include RFA as an additive tool in veterinary interventional radiology.

KEYWORDS

ex vivo, interventional radiology, radiofrequency ablation, liver, tissue morphometry, veterinary oncology

1 | INTRODUCTION

Radiofrequency ablation (RFA) consists in the local application of thermal energy by means of one or more applicators (electrodes), which produces coagulative necrosis of the adjacent tissues. Monopolar RFA systems employ a single 'active' or 'interstitial' electrode, with current dissipated at one or more return grounding pads. On the other hand, bipolar devices have two 'active' electrodes, usually placed in close proximity to achieve contiguous coagulation between them (Ahmed et al., 2014). The probe(s) emits alternative current with frequencies ranging from 450 to 500 KHz, inducing ionic agitation and producing heat. At temperatures above 60°C, cell death occurs due to protein coagulation and dehydration (Denys, De Baere, & Kuoch, 2003). Percutaneous monopolar RFA was introduced as a surgical tool in 1993 for the treatment of liver neoplasia and metastasis in human patients (Rossi et al. 1995) and it is now widely used in oncology, especially for the local treatment of hepatocellular carcinoma and hepatic metastases of colorectal cancers (Gazelle, Goldberg, and Solbiati 2000). Also, its use has been described for treating thyroid masses in human beings (Garberoglio, Aliberti, and Appetecchia 2015). A further widespread application of RFA in human medicine is for the treatment of varicose veins, for which pre-clinical swine models have been used (Badham, Dos Santos, & Whiteley, 2017; Badham, Strong, & Whiteley, 2015; Marsden, Perry, & Kelley, 2013). Therapeutic applications in veterinary medicine are limited to a few conditions described in canine patients, such as the treatment of primary hyperparathyroidism (Bucy, Pollard, and Nelson 2017), tumour masses (Martel et al., 2008) and cardiac arrhythmias (Santilli, Mateos Panero, & Porteiro Vazquez, 2018). Occasional use of RFA has been reported also for surgical procedures such as resection of the soft palate in dogs (Palierne et al. 2018). Recent studies report the evaluation of RFA ablation zones by different imaging techniques in experimental settings in healthy dogs (Lee et al. 2018; Moon et al., 2017).

Primary liver tumours in dogs account for 2% of all canine malignancies, the most frequent being hepatocellular carcinoma, which may occur as a massive, nodular and diffuse form. The latter forms usually present as multiple nodules in different liver lobes, and are not treatable with surgery. On the other hand, the massive form is often resected surgically, but the limitation may be the location on a hilar position, especially when the central or right divisions of the liver are involved. In these cases, the risk for severe haemorrhage and/or incomplete tumour resection may be relevant (Linden et al., 2019) and alternative approaches could reduce this risk. Metastatic lesions in the canine liver from non-hepatic tumours (spleen, pancreas and gastrointestinal tract) occur 2.5 times more frequently than primary tumours, but usually their surgical resection is not performed, and palliative treatment is proposed. Radiofrequency ablation could provide a suitable alternative to surgery in these scenarios. In this perspective, knowing the exact size, geometry and reproducibility of ablation zones induced by the available systems could allow a better planning of the intervention, with minimal damage to healthy tissues and reduced complications.

Radiofrequency ablation applications are usually performed under ultrasound or computer tomography guidance (Ahmed et al., 2014; Bucy et al., 2017; Oliveira Leal, Frau Pascual, & Hernandez, 2018; Padma, Martinie, & Iannitti, 2009). Ultrasound would be the most easily applicable tool for imaging-guided RFA in veterinary medicine. Ultrasound allows to determine the size of the tumour and to monitor the size of the induced ablation zone during the procedure itself. A recent report highlights that ultrasonographic imaging measurements of RFA-induced ablation zones underestimate their size however (Moon et al., 2017). Moreover, it is difficult to assess the 3 dimensional (3D) geometry of the ablation zone in real-time using ultrasound, as it provides 2 dimensional (2D) images.

Our work aimed at characterizing the size, geometry and reproducibility of the ablation zones induced by means of three different systems (generator + electrode) produced by the same company in isolated swine livers as a pre-clinical model for the dog. We investigated the effects of cold saline infusion into the liver tissue in our experiments, as it has been reported to produce larger ablation zones (Lee et al., 2004). Lastly, the effect of a single versus double passage into the parenchyma was assessed.

2 | MATERIAL AND METHODS

2.1 | Study design

The ablation zones produced using the following described five RFA conditions were tested in six isolated swine livers, namely: single passage of the internally cooled non-perfused electrode, double passage of the internally cooled non-perfused electrode, single passage of the internally cooled and perfused electrode, double passage of the internally cooled and perfused electrode, and single passage of the internally cooled electrode with a tip with adjustable exposure (from 0 to 3 cm in length), set at 1 cm.

2.2 | Livers

Six swine livers were harvested from the local abattoir and stored at 4°C until the experimental procedures were started (within 24 hr). They were left at room temperature for 2 hr before the RFA took place. Core temperature of the livers at the beginning of the RFA session was not determined.

2.3 | Radiofrequency ablation

The monopolar RF ablation systems tested consisted of a 300–500 kHz generator (RF Generator M-3004, RF Medical Co.) producing a maximum power of 200 W and one of three electrodes. A 17-gauge internally cooled, adjustable RF electrode with an exposed tip 0–30 mm (VCT-10XXB, RF Medical Co., exposed tip used at 10 mm), an 18-gauge internally cooled electrode with an exposed

tip of 10 mm (RFT-0710N, RF Medical Co.), and an 18-gauge internally cooled and perfused electrode with an exposed tip of 10 mm (RFTS1010N, RF Medical Co.) were used. Of note, the two 18-gauge electrodes differ only for their ability to infuse liquid into the tissue during the ablation procedure. Out of the three electrodes studied, two are commercialized for the treatment of thyroid nodules and one for hepatocellular carcinoma in humans (Table 1). We chose to test these specific electrodes as different dog breeds are characterized by very different sizes. While liver size in a large dog breed and in a human patient can reasonably be compared, this is not the case for the smallest canine breeds. We thus opted to study the systems used for the treatment of thyroid masses in humans, which induce ablation zones of reduced dimensions, in order to assess their potential application in the smallest canine breeds. Perfused systems allowed continuous saline infusion into the liver parenchyma during the ablation procedure. More details are provided in Table 1. Two separate circuits are present within the tip of the internally cooled and perfused electrodes. The closed circuit has the function of cooling the electrode tip. The open circuit, characterized by small apertures at the active tip of the electrode, allows infusing the tissue with fluids (i.e. isotonic or hypertonic saline) during the procedure. In our experiments, cold sterile saline solution was pumped within both circuits during RFA by means of a peristaltic pump.

Five anatomical regions were identified in the isolated livers (right lateral lobe, right medial lobe, left medial lobe, and two sites within the left lateral lobe), and the five RFA conditions described above were created once in each liver. Our experimental protocol was set to guarantee that the same RFA condition was performed only once for each anatomical region considered, with the exception of the sixth liver, where the conditions used in the first liver were repeated. This study design was thought to reduce to a minimum any effect or bias related to the liver region tested.

The procedures of RFA were performed under ultrasound (US) guidance (Figures 1 and 2a). Adhesive dispersive electrodes were used as grounding pad to close the electrical circuit and positioned under the organs tested. Maximum power was set at 80 and 120 W for 17-gauge and 18-gauge electrodes, respectively. The actual power applied was based on a negative feedback, regulated by tissue impedance. The machine was set to apply energy until the tissue conductivity dropped (due to loss of water during tissue necrosis). Tissue impedance during the procedure was measured by means of a thermocouple present on the tip of the electrode. Tissue temperature during the procedure was estimated by the system based on an algorithm, and not measured directly. Maximum power at the moment when tissue conductivity dropped and duration of energy application were recorded. Care was taken to avoid large vessels and bile ducts. When double passage (or double insertion) was performed, the electrode was withdrawn after the first RFA was performed and then replaced at a different angle as shown in Figure 1, maintaining the same entry site into the liver parenchyma. Specifically, the electrode was re-inserted at approximately a 30° angle on the plan of the ultrasound image where the ablation zone of the previous RFA could be seen.

2.4 | Morphometry

Two 21-gauge needles were then inserted parallel to the electrode tip (along the plan of the ultrasound image) and kept in place until tissue sampling was completed, in order to localize the ablated area. Using an N. 21 scalpel blade, the liver parenchyma was cut along the line connecting the needles in the attempt to divide the ablation zone into two halves along its longitudinal axis (Figure 2b). Digital photographs of the longitudinal sections of the ablation zones were acquired (Figure 2c) and morphometrical analysis was performed using Image Pro Plus (Media Cybernetics, Rockville, MD, USA). All measures were performed by the same operator, blinded to the experimental conditions. Longitudinal area ($A = r^2\ \pi$), maximal longitudinal diameter (D_{max}), minimal longitudinal diameter (D_{min}) and perimeter (Pi) of the ablation zones were measured, while their volume was estimated ($V = 1/6\ \pi\ D_{max}\ D_{min}^2$). Roundness (R, ratio between two circles that lay inside and outside each ablation zone and are tangential to it) and equivalent diameter (D_{eq}, that is the diameter of a sphere of equivalent volume) of the ablation zones were calculated. The coefficients of variation of the measures taken were calculated for all the listed parameters, grouped by ablation system, to assess the reproducibility of such system to produce similar ablation zones in different livers/liver regions. The measurements did not include biliary ducts or the reddish rim surrounding ablation.

2.5 | Statistical analysis

Statistical analyses were performed using Prism 6.0 (GraphPad Software, San Diego, CA, USA). Repeated measure two-way ANOVA with Sidak's post-test was used to assess the effect of saline

TABLE 1 Technical details of the electrodes used

Commercial ID	Internally cooled	Perfused[a]	Length of the active component	Diameter	Perfusion flow
RFT–0710N	yes	No	10 mm	18 G	—
RFTS1010N	yes	yes	10 mm	18 G	1 ml/min
VCT–10XXB	yes	no	0–30 mm (used at 10 mm)	17 G	—

[a]Perfused electrodes are those allowing for continuous saline instillation into the liver parenchyma during the RFA procedure.

perfusion (by comparing internally cooled and non-perfused versus internally cooled and perfused electrodes) and of the number of passages performed on the parameters tested. Statistical comparisons concerning the ablation zone size and geometry were performed only to compare the systems using the 18-gauge internally cooled electrode with an exposed tip of 10 mm and the 18-gauge internally cooled and perfused electrode with an exposed tip of 10 mm. The size and geometry of the ablation zones produced with the 17-gauge internally cooled, adjustable RF electrode with an exposed tip 0–30 mm used at 10 mm were only reported descriptively. The reproducibility of size and geometry of the ablation zones obtained with each system were expressed by means of the coefficient of variation of the data. Reproducibility was assessed only in ablation zones ablated with a single passage. Two-way ANOVA with Tukey's post-test was used to assess the effect of the system tested and of the parameter measured on reproducibility. *p*-values < .05 were considered as statistically significant.

3 | RESULTS

All the RFA protocols applied produced macroscopically appreciable ablation zones in the liver parenchyma, identified as pale oval-shaped areas consisting of friable tissue (Figure 2c). Maximal power reached during RFA application was 45 W with the 17-gauge electrode system (range: 40–45 W), and 80 W for both 18-gauge electrode systems (range: 45–80 W). A drop in tissue conductivity was reached after a maximum time of 12 min with the 17-gauge electrode system (range: 10–12 min), and after a maximum of 30 s with both 18-gauge electrode systems (ranges: 9–30 s for the internally cooled and perfused system and 25–30 s for the internally cooled and non-perfused system). A darker zone was identifiable in the centre of the ablation zones ('charring'), where the needle was positioned. Also, a reddish rim was present around the ablation zones.

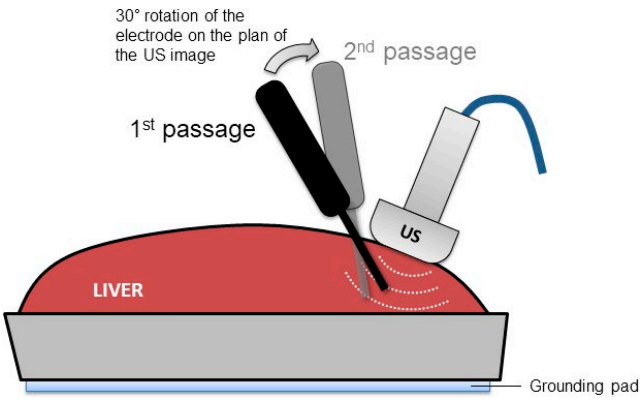

FIGURE 1 Double passage ablation

3.1 | Effect of saline perfusion and single versus. double passage

The effects of continuous saline perfusion (internally cooled and non-perfused versus internally cooled and perfused system) and of double versus single passage on size and geometry of the ablated zones produced by the systems using the 18-gauge internally cooled electrode with an exposed tip of 10 mm and the 18-gauge internally cooled and perfused electrode with an exposed tip of 10 mm are reported in Figure 3. Briefly, we observed a significant effect of the number of passages performed (p = .005) on the estimated volume of the ablation zone. A significant interaction was also observed between the number of passages performed and saline perfusion (p = .04). At the conditions tested, the estimated volume of the ablation zone was significantly increased with saline perfusion only when double passage was performed (p = .01). A similar trend was also observed for minimal longitudinal diameter, where a significant effect of the number of passages performed was observed (p = .002) but the interaction with saline perfusion was not significant (p = .06). Maximal longitudinal diameter was significantly affected only by saline perfusion (p = .008), while equivalent diameter only by the number of passages (p = .04). No effect of saline or number of passages was noticed on estimated roundness index.

3.2 | Reproducibility of the ablated zones

The size and geometry of the ablated zones induced by a single passage within the liver parenchyma of the three systems tested are reported in Table 2, together with the coefficients of variation for

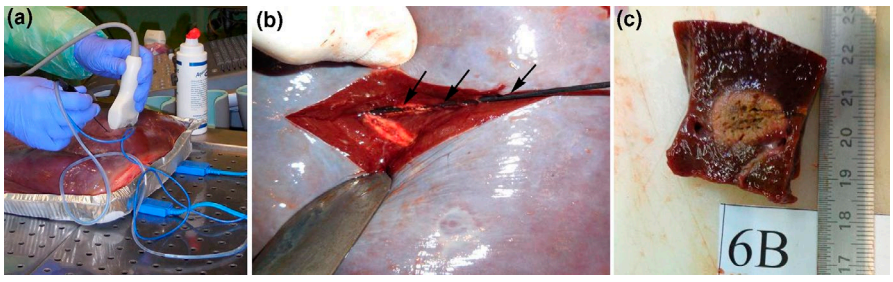

FIGURE 2 Application of RFA on isolated livers. (a) The procedure is performed under US guidance. (b) Liver tissue is cut along the longitudinal axis of the ablation zone, where the electrode was inserted during the RFA procedure (arrows). (c) The ablation zone within the liver parenchyma is identifiable as a discoloured and friable portion of liver parenchyma

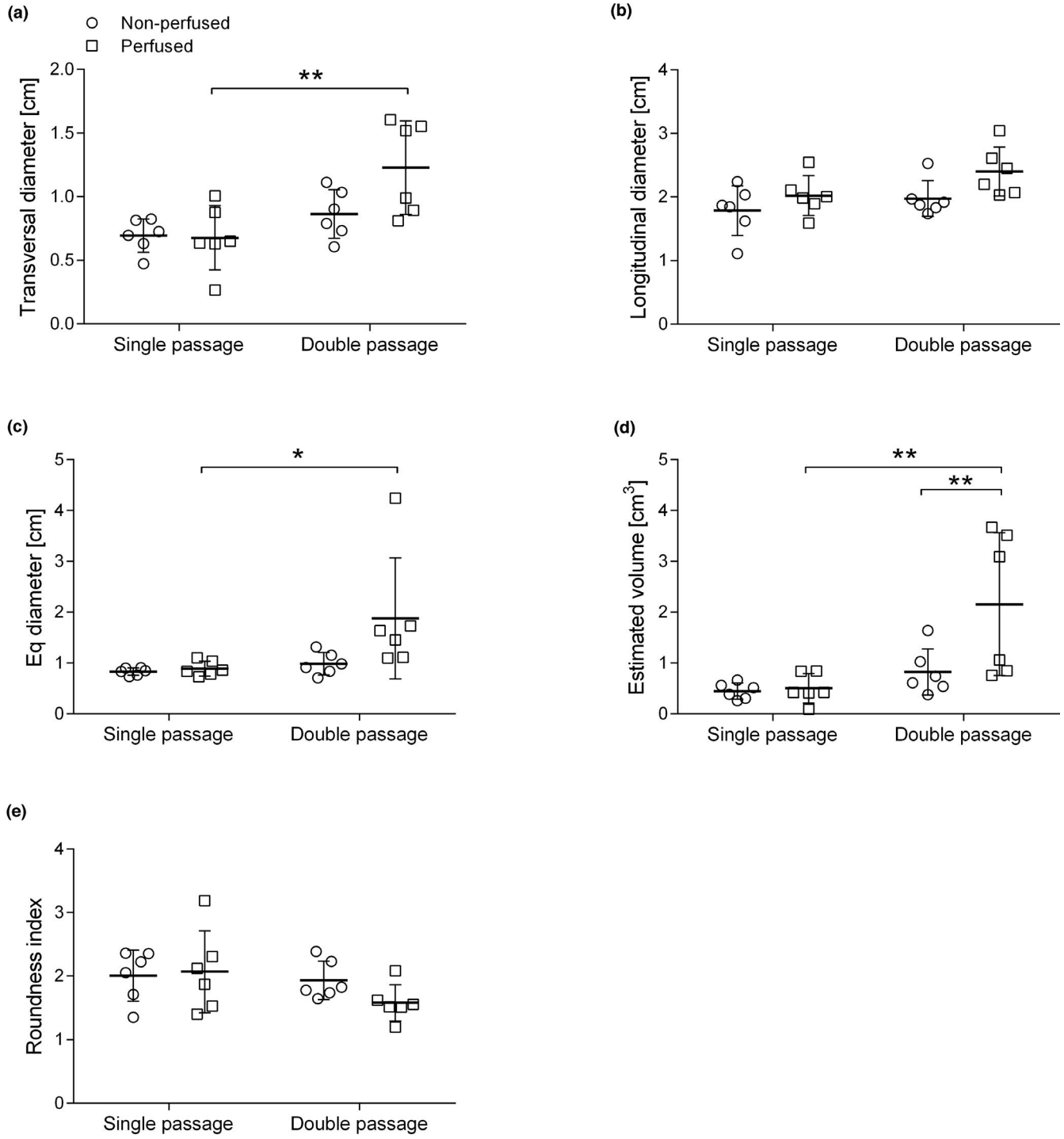

FIGURE 3 Effect of saline perfusion and of double versus. single passage on ablation zone size and geometry. (a) Transversal diameter. (b) Longitudinal diameter. (c) Equivalent diameter. (d) Estimated volume. (e) Estimated roundness index. *p < .05 (post-test). **p < .01 (post-test)

each parameter, which is the index we used to describe reproducibility. Overall, statistical analysis revealed a significant effect of the parameters measured (p = .005) but not of the electrodes tested (p = .3) on reproducibility. The reproducibility was lower for estimated volume measures compared with all other parameters tested (significantly higher coefficients of variation; p < .05).

The data that support the findings of this study are available from the corresponding author upon reasonable request.

4 | DISCUSSION

RFA is a minimally invasive technique widely used in human interventional radiology, especially for the treatment of local tumour or metastasis (Gazelle et al., 2000). Different RFA systems are commercially available and frequently employed in clinical practice, although product-specific, standardized data on achievable ablation dimensions in different tissues are often missing from the manufacturers.

TABLE 2 Reproducibility of the ablation zones ablated with a single passage

Electrode	Area [cm^2]	D_{max} [cm]	D_{min} [cm]	D_{eq} [cm]	Pi [cm]	R [-]	Vol [cm^3]
RFT–0710N	0.19 (1.05 ± 0.2)	0.22 (1.79 ± 0.39)	0.19 (0.69 ± 0.13)	0.09 (0.83 ± 0.07)	0.19 (5.10 ± 0.96)	0.20 (2.01 ± 0.40)	0.35 (0.45 ± 0.16)
RFTS1010N	0.12 (1.21 ± 0.14)	0.15 (2.02 ± 0.31)	0.37 (0.68 ± 0.25)	0.17 (0.89 ± 0.15)	0.17 (5.52 ± 0.93)	0.31 (2.07 ± 0.65)	0.57 (0.51 ± 0.29)
VCT–10XXB	0.35 (5.60 ± 1.98)	0.22 (3.52 ± 0.76)	0.18 (1.85 ± 0.34)	0.19 (2.19 ± 0.42)	0.19 (10.06 ± 1.93)	0.19 (1.49 ± 0.29)	0.55 (6.84 ± 3.78)
Mean CV	0.22[a]	0.20[a]	0.25[a]	0.15[b]	0.18[b]	0.23[a]	0.49

Note: Results are expressed as CV (mean ± S.D).

Abbreviations: CV, coefficient of variation; D_{max}, longitudinal diameter; D_{min}, transversal diameter; D_{eq}, equivalent diameter; Pi, perimeter; R, estimated roundness; Vol, estimated volume.

[a]Significantly different from the CV of estimated volume data ($p < .05$).

[b]Significantly different from the CV of estimated volume data ($p < .01$).

Interventional radiology is an emerging discipline in veterinary medicine, with few reports of RFA applications in companion animals. The non-invasiveness and rapidity of execution associated with this technique make it a possible choice for the ablation of canine liver masses located in regions difficult to reach, possibly reducing the morbidity and post-operative hospitalization time associated with these interventions (Linden et al., 2019). Using isolated swine livers as a pre-clinical model, our study has described the size, geometry and reproducibility of the ablation zones induced by three commercially available systems commonly employed in the treatment of thyroid nodules (RFT-0710N and RFTS1010N, RF Medical Co.) or hepatocellular carcinoma (VCT-10XXB, RF Medical Co.) in humans. The dielectric properties of freshly isolated swine liver resemble those commonly encountered in liver tumours, justifying their choice for this type of experimental approach (Stauffer, Rossetto, & Prakash, 2003). The data obtained may reveal helpful in the future for veterinary oncologists and/or interventional radiologists in order to plan and propose RFA treatment for selected cases of liver tumours.

Overall, our data indicate that internally cooled and perfused systems produce larger ablation zones compared with internally cooled and non-perfused systems. This is in line with previous reports (Lee, Kim, & Han, 2005; Livraghi et al., 1997). Continuous perfusion of saline into the tissue through holes at the extremity of the electrode increases the electrical conductivity of the tissue adjacent to the electrode tip, thus increasing RF ablation zone size (Denys et al., 2003). The conductivity of 0.9% saline solution is 12–15 times higher than that of the soft tissues, and conductivity increases with increasing saline concentration (Miao et al., 2001). Of note, isotonic saline was used as a perfusion fluid in our study, which could have reduced the effects of the internally cooled and perfused systems in terms of ablation zone size compared with studies using hypertonic saline (Lee et al., 2005). In spite of the significant effect of saline infusion on the estimated volume of the ablation zones produced by perfused versus non-perfused systems, statistically significant differences were observed only when double passage was performed. This also could be due to the fact that isotonic saline was employed, joined to the short time required to the system to make tissue conductivity drop. With saline being pumped at 1 ml/min, ablation times as short as 9 s as those observed for cooled and perfused systems resulted in volumes as small as 0.2 ml being infused.

The reproducibility of the ablation zones induced with the systems tested was considered as acceptable in our study. We observed CVs ranging from 0.09 to 0.37 (mean 0.20) for lineal measurements as diameters, which is in line with previous reports (Song et al., 2015). It also has to be acknowledged that this variation was likely caused by other factors that summed up to the specific performance variability of the systems tested. Indeed, the ablation zones were intentionally induced in different liver zones in our study, which very likely contributed to the variability observed. We believe this approach more closely resembles what occurs in real clinical life. The CVs of volume measures were higher, ranging from 0.35 to 0.57 (mean: 0.49). This might be due to the fact that bidimensional measures do not allow an accurate estimation of volumes, for which different approaches will have to be used in future studies.

Our data were obtained ex vivo, using macroscopically healthy livers. We are aware that in vivo and in the presence of neoplastic tissue these results could be altered (Denys et al., 2003). Previous studies have reported larger ablation zones in patients with hepatic tumors compared with healthy livers, which is likely attributable to the difference between hepatic and tumor perfusion (Montgomery, Rahal, & Dodd, 2004). The passive centrifugal diffusion of heat from the active radiofrequency energy heating zone accounts, by far, for most of the final ablation volume. Such passive heat diffusion is extremely sensitive to the cooling effect generated by tissue microvascularization (commonly known as the 'heat sink effect')(Lu et al., 2002) and macrovessel blood flow at the tumor and non-tumour interface (Seror, 2014). Further in vivo studies on veterinary patients are warranted to confirm our findings. Moreover, we estimated ablation volumes by analysing macroscopic photographs taken only from a single slice. While evidence exists in support of the use of gross pathological examination as a reliable indicator of lethally damaged tissue in RFA (Gemeinhardt et al., 2016; Song et al., 2017), a real 3D ablation analysis (either performed by multi

slice histology, macroscopy or CT) might have improved the accuracy of our results and should be preferred for the assessment of in vivo ablated zones.

In conclusion, we have characterized the size, geometry and reproducibility of the ablation zones obtained using three commercially available systems, which could be helpful for veterinary oncologists and interventional radiologists for an optimal planning of their interventions. Our data support the use of internally cooled and isotonic saline-perfused rather than internally cooled systems to induce larger RFA ablation zones when the same power is applied to the tissues.

ACKNOWLEDGEMENTS

The Authors would like to thank RF Medical Co., Ltd. (Korea), which kindly provided the instrumentation for performing the experiments.

CONFLICT OF INTEREST

The Authors declare they have no conflict of interest.

AUTHOR CONTRIBUTION

Michela Bullone: Data curation; Formal analysis; Methodology; Writing-original draft; Writing-review & editing. **Roberto Garberoglio:** Conceptualization; Methodology; Supervision; Writing-review & editing. **Paola Pregel:** Conceptualization; Data curation; Methodology; Supervision; Writing-review & editing. **Francesca Tiziana Cannizzo:** Conceptualization; Supervision; Writing-review & editing. **Arianna Gagliardo:** Data curation; Methodology; Writing-review & editing. **Marina Martano:** Conceptualization; Supervision; Writing-review & editing. **Enrico Bollo:** Conceptualization; Supervision; Writing-review & editing. **Frine Eleonora Scaglione:** Conceptualization; Funding acquisition; Project administration; Supervision; Writing-review & editing.

ORCID

Michela Bullone https://orcid.org/0000-0002-9094-6734

PEER REVIEW STRATEMENT

The peer review history for this article is available at https://publons.com/publon/10.1002/vms3.319

REFERENCES

Ahmed, M., Solbiati, L., Brace, C. L., Breen, D. J., Callstrom, M. R., & Charboneau, J. W. ... Standard of Practice Committee of the Cardiovascular and Interventional Radiological Society of Europe. (2014). Image-guided tumor ablation: Standardization of terminology and reporting criteria–a 10-year update. *Journal of Vascular and Interventional Radiology*, *25*(11), 1691–705 e4.

Badham, G. E., Dos Santos, S. J., & Whiteley, M. S. (2017). Radiofrequency-induced thermotherapy (RFiTT) in a porcine liver model and ex vivo great saphenous vein. *Minimally Invasive Therapy and Allied Technologies*, *26*(4), 200–206.

Badham, G. E., Strong, S. M., & Whiteley, M. S. (2015). An in vitro study to optimise treatment of varicose veins with radiofrequency-induced thermo therapy. *Phlebology*, *30*(1), 17–23.

Bucy, D., Pollard, R., & Nelson, R. (2017). Analysis of factors affecting outcome of ultrasound-guided radiofrequency heat ablation for treatment of primary hyperparathyroidism in dogs. *Veterinary Radiology & Ultrasound*, *58*(1), 83–89. https://doi.org/10.1111/vru.12451

Denys, A. L., De Baere, T., Kuoch, V. et al (2003). Radio-frequency tissue ablation of the liver: In vivo and ex vivo experiments with four different systems. *European Radiology*, *13*(10), 2346–2352. https://doi.org/10.1007/s00330-003-1970-0

Garberoglio, R., Aliberti, C., Appetecchia, M. et al (2015). Radiofrequency ablation for thyroid nodules: Which indications? The first Italian opinion statement. *Journal of Ultrasound*, *18*(4), 423–430. https://doi.org/10.1007/s40477-015-0169-y

Gazelle, G. S., Goldberg, S. N., Solbiati, L., Livraghi, T. (2000). Tumor ablation with radio-frequency energy. *Radiology*, *217*(3), 633–646. https://doi.org/10.1148/radiology.217.3.r00dc26633

Gemeinhardt, O., Poch, F. G., Hiebl, B., Kunz-Zurbuchen, U., Corte, G. M., Thieme, S. F., ... Lehmann, K. S. (2016). Comparison of bipolar radiofrequency ablation zones in an in vivo porcine model: Correlation of histology and gross pathological findings. *Clin Hemorheol Microcirc*, *64*(3), 491–499. https://doi.org/10.3233/CH-168123

Lee, D., Park, S., Ang, M. J. C., Park, J.-G., Yoon, S., Kim, C., ... Choi, J. (2018). Evaluation of liver lesions by use of shear wave elastography and computed tomography perfusion imaging after radiofrequency ablation in clinically normal dogs. *American Journal of Veterinary Research*, *79*(11), 1140–1149. https://doi.org/10.2460/ajvr.79.11.1140

Lee, J. M., Han, J. K., Kim, S. H., Lee, J. Y., Shin, K. S., Han, C. J., ... Choi, B. I. (2004). Optimization of wet radiofrequency ablation using a perfused-cooled electrode: A comparative study in ex vivo bovine livers. *Korean J Radiol*, *5*(4), 250–257. https://doi.org/10.3348/kjr.2004.5.4.250

Lee, J. M., Kim, S. H., Han, J. K., Sohn, K. L., & Choi, B. I. (2005). Ex vivo experiment of saline-enhanced hepatic bipolar radiofrequency ablation with a perfused needle electrode: Comparison with conventional monopolar and simultaneous monopolar modes. *Cardiovascular and Interventional Radiology*, *28*(3), 338–345. https://doi.org/10.1007/s00270-004-0177-3

Linden, D. S., Liptak, J. M., Vinayak, A., Cappelle, K., Hoffman, C., Fan, S., ... Matz, B. M. (2019). Outcomes and prognostic variables associated with central division hepatic lobectomies: 61 dogs. *Veterinary Surgery*, *48*(3), 309–314. https://doi.org/10.1111/vsu.13164

Livraghi, T., Goldberg, S. N., Monti, F., Bizzini, A., Lazzaroni, S., Meloni, F., ... Gazelle, G. S.. (1997). Saline-enhanced radio-frequency tissue ablation in the treatment of liver metastases. *Radiology*, *202*(1), 205–210. https://doi.org/10.1148/radiology.202.1.8988212

Lu, D. S., Raman, S. S., Vodopich, D. J., Wang, M., Sayre, J., & Lassman, C. (2002). Effect of vessel size on creation of hepatic radiofrequency lesions in pigs: assessment of the "heat sink" effect. *AJR American Journal of Roentgenology*, *178*(1), 47–51. https://doi.org/10.2214/ajr.178.1.1780047

Marsden, G., Perry, M., Kelley, K., Davies, A. H.. (2013). Diagnosis and management of varicose veins in the legs: Summary of NICE guidance. *BMJ*, *347*, f4279. https://doi.org/10.1136/bmj.f4279

Martel, J., Bueno, A., Dominguez, M. P., Llorens, P., Quirós, J., & Delgado, C. (2008). Percutaneous radiofrequency ablation: Relationship between different probe types and procedure time on length and extent of osteonecrosis in dog long bones. *Skeletal Radiology*, *37*(2), 147–152. https://doi.org/10.1007/s00256-007-0416-1

Miao, Y., Ni, Y., Yu, J., Zhang, H., Baert, A., & Marchal, G. (2001). An ex vivo study on radiofrequency tissue ablation: Increased lesion size by using an "expandable-wet" electrode. *European Radiology*, *11*(9), 1841–1847. https://doi.org/10.1007/s003300100891

Montgomery, R. S., Rahal, A., Dodd, G. D. 3rd, Leyendecker, J. R., & Hubbard, L. G. (2004). Radiofrequency ablation of hepatic tumors: Variability of lesion size using a single ablation device. *AJR American Journal of Roentgenology*, *182*(3), 657–661.

Moon, S., Park, S., Lee, S. K., Cheon, B., Hong, S., Cho, H., ...Choi, J. (2017). Comparison of elastography, contrast-enhanced ultrasonography, and

computed tomography for assessment of lesion margin after radiofrequency ablation in livers of healthy dogs. *American Journal of Veterinary Research*, *78*(3), 295–304. https://doi.org/10.2460/ajvr.78.3.295

Oliveira Leal, R., Frau Pascual, L., & Hernandez, J. (2018). The Use of percutaneous ultrasound-guided radiofrequency heat ablation for treatment of primary hyperparathyroidism in eight dogs: Outcome and complications. *Veterinary Sciences*, *5*(4), 91–https://doi.org/10.3390/vetsci5040091

Padma, S., Martinie, J. B., & Iannitti, D. A. (2009). Liver tumor ablation: Percutaneous and open approaches. *Journal of Surgical Oncology*, *100*(8), 619–634. https://doi.org/10.1002/jso.21364

Palierne, S., Meynaud, P., Bilmont, A., Delverdier, M., Semin, M.-O., Stieglitz, M., … Autefage, A. (2018). Plasma-mediated bipolar radiofrequency ablation of overlong soft palate in the dog: A pilot study. *Journal of the American Animal Hospital Association*, *54*(5), 267–275. https://doi.org/10.5326/JAAHA-MS-6668

Rossi, S., Di Stasi, M., Buscarini, E., Cavanna, L., Quaretti, P., Squassante, E., … Buscarini, L. (1995). Percutaneous radiofrequency interstitial thermal ablation in the treatment of small hepatocellular carcinoma. *The Cancer Journal from Scientific American*, *1*(1), 73–81.

Santilli, R. A., Mateos Panero, M., Porteiro Vazquez, D. M., Perini, A., & Perego, M. (2018). Radiofrequency catheter ablation of accessory pathways in the dog: The Italian experience (2008–2016). *Journal of Veterinary Cardiology*, *20*(5), 384–397. https://doi.org/10.1016/j.jvc.2018.07.006

Seror, O. (2014). Percutaneous hepatic ablation: What needs to be known in 2014. *Diagnostic and Interventional Imaging*, *95*(7–8), 665–675. https://doi.org/10.1016/j.diii.2014.04.002

Song, K. D., Lee, M. W., Park, H. J., Cha, D. I., Kang, T. W., Lee, J., … Rhim, H. (2015). Hepatic radiofrequency ablation: In vivo and ex vivo comparisons of 15-gauge (G) and 17-G internally cooled electrodes. *British Journal of Radiology*, *88*(1050), 20140497.

Song, K. D., Lee, M. W., Rhim, H., Kang, T. W., Cha, D. I., & Yang, J. (2017). Chronological changes of radiofrequency ablation zone in rabbit liver: An in vivo correlation between gross pathology and histopathology. *British Journal of Radiology*, *90*(1071), 20160361.

Stauffer, P. R., Rossetto, F., Prakash, M., Neuman, D. G., & Lee, T. (2003). Phantom and animal tissues for modelling the electrical properties of human liver. *International Journal of Hyperthermia*, *19*(1), 89–101. https://doi.org/10.1080/0265673021000017064

How to cite this article: Bullone M, Garberoglio R, Pregel P, et al. Characterization of the ablation zones produced by three commercially available systems from a single vendor for radiofrequency thermoablation in an ex vivo swine liver model. *Vet Med Sci*. 2020;6:1041–1048. https://doi.org/10.1002/vms3.319